Disturbance Observer-Based Neural Network Control of Cooperative Multiple Manipulators with Input Saturation

Wei He, Yongkun Sun, Zichen Yan, Chenguang Yang, Zhijun Li, Okyay Kaynak

***Abstract*—In this paper, the complex problems of internal forces and position control are studied simultaneously and a disturbance observer-based radial basis function neural network (RBFNN) control scheme is proposed to (i) estimate the unknown parameters accurately, (ii) approximate the disturbance experienced by the system due to input saturation, (iii) simultaneously improve the robustness of the system. More specifically, the proposed scheme utilizes disturbance observers, neural network (NN) collaborative control with an adaptive law, and full state feedback. Utilizing Lyapunov stability principles, it is shown that semi-globally uniformly bounded stability is guaranteed for all controlled signals of the closed-loop system. The effectiveness of the proposed controller as predicted by the theoretical analysis is verified by comparative experimental studies.**

***Index Terms*—Adaptive neural network control, multi-manipulator collaborative control, distubance observer, input saturation, robot.**

I. Introduction

In three-dimensional task space, compared with a single manipulator, cooperative multiple manipulators (CMM) have more conspicuous advantages in the carriage of heavy objects, the assembly of intricate parts, and the interaction between people and robots [1]–[3]. In recent years, CMM, rather than a single manipulator, have been more widely employed in service robots and industrial robots market, because CMM possess the ability of greater flexibility, higher reliability, and larger payload capacity to accomplish more complex industrial tasks. Simultaneously, great progress has been made in the nonlinear intelligent control algorithms [4]–[12]. However, there still exist a sequence of crucial issues about CMM that need to be pondered. For example, if position errors are relatively large, huge internal forces may be produced that can damage handled objects or manipulators themselves.

W. He, Y. Sun and Z. Yan are with the School of Automation and Electrical Engineering, the Institute of Artificial Intelligence, University of Science and Technology Beijing, Beijing 100083, China. (*Corresponding author: Wei He, Email: weihe@ieee.org*)

C. Yang is with Bristol Robotics Laboratory, University of the West of England, Bristol, BS16 1QY, UK.

Z. Li is with the Department of Automation, University of Science and Technology of China, Hefei 230026, China.

O. Kaynak is with the School of Automation and Electrical Engineering, University of Science and Technology Beijing, Beijing 100083, China and also with Bogazici University, Istanbul 34342, Turkey.

This work was supported in part by the National Natural Science Foundation of China under Grant 61873298, in part by the Beijing Natural Science Foundation under Grant 4172041, and in part by the Joint Funds of Equipment Pre-Research and Ministry of Education of China under Grant 6141A02033339, and in part by Engineering and Physical Sciences Research Council (EPSRC) under Grant EP/S001913.

Due to the size and the weight of large objects, some closed-chain tasks may have to be accomplished through a multi-manipulator system. Therefore, the design of an effective multi-manipulator cooperative control strategy is of great significance in the industry. However, in comparison with a single robot system, multi-manipulator robots have great differences in the solution of the kinematics and the analysis of the dynamic model [13]. In [14]–[16], the authors put forward methods for trajectory tracking of end effectors and the relationship of interaction forces. The interaction between the payload and the manipulators is usually described by an impedance model in [17]–[19]. To tackle the motion and force problems, a decentralized coordination control scheme is suggested in this paper. In a decentralized control architecture [20], each manipulator is controlled independently by its own controller. The decentralized control scheme has less computation cost. The control laws for all the manipulators can be the same, while no communication is needed between them.

For a robot manufacturer, kinematic parameters of robots can innately be known, but there exist the problems of unavailable external disturbances and uncertainties in the dynamic model of a robot system [21]–[24]. Unlike traditional methods, artificial intelligence based control methods have the advantages of not requiring accurate models [25]–[29]. A method, which can reduce the requirements of robotic manipulator parameters, was taken into account in the feedback control presented in [30]–[35]. In [36]–[39], NN controllers by full state feedback were adopted to achieve trajectory-tracking control of manipulators with unknown dynamic parameters. These efforts were complemented by an adaptive NN control strategy implemented in [40]–[42], to compensate the uncertainties generated by the external environment, the interaction between manipulators and objects, and the inexactness in dynamic parameters of the manipulators. Compared with other NN control methods, RBFNN is a local approximation network and has no local minimum problem [43]. Consequently, it performs better in approximating the unknown model.

All actuators have an upper bound of torque. When it is reached, non-linear saturation of the motor can affect the instantaneous performance of the system, resulting in its instability [44]–[46]. Input saturation in a multi-manipulator robot system cannot be neglected in controller design. A second key question is how to deal with input saturation in CMM, to ensure that the joint angles track the desired trajectory in a reasonable space. Various approaches have been suggested in connection with input saturation. In [47], with regard to uncertainties in robotic systems and the potential actuator saturation, the authors proposed a saturated adaptive robust control strategy. In [48], Nussbaum function was recommended to make up for the non-linear term generated by the input saturation and external disturbance, which did not require assumptions on uncertain parameters within a known compact set. In [49] and [50], an adaptive fuzzy control method was proposed for a class of uncertain nonstrict-feedback systems with input saturation and output constraints while this paper proposed an adaptive RBFNN technique.

External disturbances in the environment may introduce uncertainties to manipulators that may cause large tracking errors and threaten the safety of the robotic manipulators and the surrounding people [51]–[53]. So a third key question is how to design a disturbance observer and simultaneously guarantee the stability of the system [54]–[57]. In [58], adaptive fuzzy controllers by state feedback and output feedback combining with fuzzy approximation and disturbance observers have been presented to estimate existing uncertainties of dynamic parameters, unknown input saturation, and unknown external disturbances. An innovative control method that combines human-operated control and robot automatic control was proposed in [59]. Nevertheless, the approaches briefly reviewed above find it hard to compensate for all uncertainties. In [60]–[62], a nonlinear disturbance-observer-based control approach is proposed to improve the robust performance for a nonlinear system. The present work is motivated by this fact. To neutralize the uncertainties discussed, RBFNN controllers with parameter adaptation mechanisms and disturbance observers that provide information on torque inputs are inserted into the system via feed-forward loops.

There are numerous methods for stability analysis of NNs described in the literature, e.g. [63]–[66]. In this particular paper, through the Lyapunov stability analysis, it is ascertained that the stability of the multi-manipulator robot system is guaranteed and the boundedness of the system state variables is achieved by choosing appropriate control gains, especially tracking errors of link angles which converges to little neighborhoods in input saturation defined by authors.

This manuscript is arranged as follows. N-link non-linear CMM system dynamic model used in this study is demonstrated in Section II. The control design and the stability proof via Lyapunov stability theorem are discussed in Section III. A series of control experiments are presented. The feasibility and the effectiveness of the proposed controllers are verified in Section IV by a comparative study with PID control and NN control with the rigid manipulator model. At the end of the paper, in Section V, we summarize the research results.

II. Preliminaries and Problem Formulation

A multi-manipulator robot grasping a normal object is proposed to implement a special task as shown in Fig. 1.

A. Problem Formulation

1) Kinematics of system: We can define the kinematic description of an end effector $q_b = [q_{(p)}, q_{(o)}] \in \mathbb{R}^{N_o}$, where $q_{(p)}$ and $q_{(o)}$ present the position and the orientation with regard to the reference coordinate system, respectively and N_o is the degree of freedom (DOF) of the object [67]. The forward kinematics function Φ_i converts the joint angle q_{m_i} to the description of position and orientation q_b, so we can get the forward kinematics

$$q_b = \Phi_i(q_{m_i}). \tag{1}$$

where the number of manipulators $i = 1, 2, \ldots, r$. Differentiating (1) with respect to time, we can get derivatives of q_b

$$\dot{q}_b = \dot{\Phi}_i(q_{m_i}) = J_{\Phi_i}(q_{m_i})\dot{q}_{m_i} \tag{2}$$

$$\ddot{q}_b = \dot{J}_{\Phi_i}(q_{m_i})\dot{q}_{m_i} + J_{\Phi_i}(q_{m_i})\ddot{q}_{m_i} \tag{3}$$

where J_{Φ_i} represents the Jacobian matrix, $\dot{q}_{m_i} \in \mathbb{R}^{N_i}$ and $\ddot{q}_{m_i} \in \mathbb{R}^{N_i}$ represent joint velocity and joint acceleration of the ith manipulator and N_i is DOF of the ith manipulator.

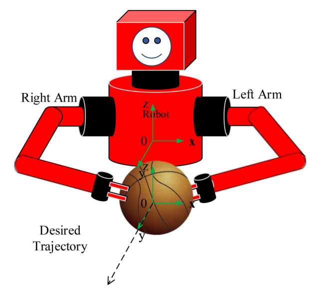

Fig. 1: A multi-manipulator robot grabbing movement along the reference trajectory.

2) Dynamics of system: The dynamic equation of the ith manipulator [68] in the joint space is given as

$$\begin{aligned} M_{m_i}(q_{m_i})\ddot{q}_{m_i} + C_{m_i}(q_{m_i}, \dot{q}_{m_i})\dot{q}_{m_i} + G_{m_i}(q_{m_i}) = \\ Sat(\tau_i) - f_{dis_i} + J_{e_i}^T(q_{m_i})F_{e_i}, \quad i = 1, 2, \ldots, r \end{aligned} \tag{4}$$

where $M_{m_i}(q_{m_i}) \in \mathbb{R}^{N_i \times N_i}$, $C_{m_i}(q_{m_i}, \dot{q}_{m_i})\dot{q}_{m_i} \in \mathbb{R}^{N_i}$, and $G_{m_i}(q_{m_i}) \in \mathbb{R}^{N_i}$ are the inertia matrix, the Centripetal and Corilis force, and the gravitational force vector of the ith robotic manipulator, respectively. J_{e_i} denotes Jacobian matrix of the ith robotic manipulator. τ_i and F_{e_i} represent the joint torque vector and the force applied to the end effector. $Sat(\tau_i)$ denotes the joint torque vector with input saturation. $Sat(\tau_i)$ can be described as

$$Sat(\tau_i) = \begin{cases} S_{\max}\text{sign}(\tau_i) & |\tau_i| \geq S_{\max} \\ \tau_i & |\tau_i| < S_{\max}. \end{cases} \tag{5}$$

The dynamic equation of the grasped object [69] is

$$M_b(q_b)\ddot{q}_b + C_b(q_b, \dot{q}_b)\dot{q}_b + G_b(q_b) = F_b \tag{6}$$

where $M_b(q_b)$, $C_b(q_b, \dot{q}_b)\dot{q}_b$ and $G_b(q_b)$ are the inertia matrix, the Centripetal and Corilis force, and the gravitational force vector of the grasped object, respectively. F_b is the resultant force applied on the center of gravity of the object. F_b can be formed from

$$F_b = -\sum_{i=1}^{r} F_{be_i}, \;\; F_{be_i} = J_{be_i}^T(q_b)F_{e_i}, \;\; F_{be_i} = f_{I_i} + f_{E_i} \tag{7}$$

where F_{be_i} represents the counterforce exerted by an object to the end effector of the ith robotic manipulator and consists of an interal force f_{I_i} and an external force f_{E_i}, and internal forces offset each other $\sum_{i=1}^{r} f_{I_i} = 0$. The relationship among $J_{\Phi_i}(q_{m_i})$, $J_{e_i}(q_{m_i})$ and $J_{be_i}(q_b)$ is showed as $J_{e_i}(q_{m_i}) = J_{be_i}(q_b)J_{\Phi_i}(q_{m_i})$. Combining (6) and (7), the dynamic equation of the object becomes

$$M_b(q_b)\ddot{q}_b + C_b(q_b, \dot{q}_b)\dot{q}_b + G_b(q_b) = -\sum_{i=1}^{r} f_{E_i}. \tag{8}$$

Therefore, we have

$$f_{E_i} = -Q_i(t)\big(M_b(q_b)\ddot{q}_b + C_b(q_b, \dot{q}_b)\dot{q}_b + G_b(q_b)\big) \tag{9}$$

where $Q_i \in \mathbb{R}^{N_o \times N_o}$ is the load distribution diagonal matrix meeting $\sum_{i=1}^{r} Q_i = I$. So taking (2), (3) and (9) into F_{be_i} in (7) yields

$$\begin{aligned} F_{be_i} =& -Q_i(t)\Big(M_b(q_b)\big(\dot{J}_{\Phi_i}(q_{m_i})\dot{q}_{m_i} + J_{\Phi_i}(q_{m_i})\ddot{q}_{m_i}\big) \\ &+ C_b(q_b, \dot{q}_b)J_{\Phi_i}(q_{m_i})\dot{q}_{m_i} + G_b(q_b)\Big) + f_{I_i}. \end{aligned} \tag{10}$$

Combining the relationship between the Jacobian matrices and (10) yields

$$\begin{aligned} J_{e_i}^T(q_{m_i})F_{e_i} =& J_{\Phi_i}^T(q_{m_i})J_{be_i}^T(q_b)F_{e_i} \\ =& J_{\Phi_i}^T(q_{m_i})F_{be_i} \\ =& -Q_i(t)J_{\Phi_i}^T(q_{m_i})\big[M_b(q_b)\big(\dot{J}_{\Phi_i}(q_{m_i})\dot{q}_{m_i} \\ &+ J_{\Phi_i}(q_{m_i})\ddot{q}_{m_i}\big) + C_b(q_b, \dot{q}_b)J_{\Phi_i}(q_{m_i})\dot{q}_{m_i} \\ &+ G_b(q_b)\big] + J_{\Phi_i}^T(q_{m_i})f_{I_i}. \end{aligned} \tag{11}$$

Then substituting (11) into (4), we have

$$\begin{aligned} Sat(\tau_i) =& \big[M_{m_i}(q_{m_i}) + Q_i(t)J_{\Phi_i}^T(q_{m_i})M_b(q_b)J_{\Phi_i}(q_{m_i})\big]\ddot{q}_{m_i} \\ &+ \big[C_{m_i}(q_{m_i}, \dot{q}_{m_i}) + Q_i(t)J_{\Phi_i}^T(q_{m_i})\big(M_b(q_b) \\ &\times \dot{J}_{\Phi_i}(q_{m_i}) + C_b(q_b, \dot{q}_b)J_{\Phi_i}(q_{m_i})\big)\big]\dot{q}_{m_i} \\ &+ \big[G_{m_i}(q_{m_i}) + Q_i(t)J_{\Phi_i}^T(q_{m_i})G_b(q_b)\big] \\ &- J_{\Phi_i}^T(q_{m_i})f_{I_i} + f_{dis_i}. \end{aligned} \tag{12}$$

The cooperative dynamic equation of the robot and the object is rewritten as

$$\begin{aligned} M_{c_i}(q_{m_i})\ddot{q}_{m_i} + C_{c_i}(q_{m_i}, \dot{q}_{m_i})\dot{q}_{m_i} + G_{c_i}(q_{m_i}) \\ + f_{dis_i} - J_{\Phi_i}^T(q_{m_i})f_{I_i} = Sat(\tau_i) \end{aligned} \tag{13}$$

where $M_{c_i} = M_{m_i} + Q_iJ_{\Phi_i}^TM_bJ_{\Phi_i}, C_{c_i} = C_{m_i} + Q_iJ_{\Phi_i}^T\big(M_b \times \dot{J}_{\Phi_i} + C_bJ_{\Phi_i}\big), G_{c_i} = G_{m_i} + Q_iJ_{\Phi_i}^TG_b$.

B. Assumptions and Properties

Assumption 1: [70] When the object is grasped by the arms, there exists no relative movement between the end effector and the object.

Assumption 2: [70] The object does not deform obviously due to the force exerted by the arms.

Assumption 3: [68] The disturbance $f_{dis_i}(t)$ is assumed to be continuous because it can be largely attributed to the exogenous effects; $f_{dis_i}(t)$ has finite energy and meets $\| f_{dis_i}(t) \| \leq f_M$, where f_M is an unknown positive constant.

Property 1: [71] The matrix $\dot{M}_{c_i}(q_{m_i}) - 2C_{c_i}(q_{m_i}, \dot{q}_{m_i}) - \dot{Q}_i(t)J_{\Phi_i}^T(q_{m_i})M_b(q_b)J_{\Phi_i}(q_{m_i})$ is skew-symmetric.

$$\begin{aligned} \forall \nu \in \mathbb{R}^{N_i},\ \nu^T\{\dot{M}_{c_i}(q_{m_i}) - 2C_{c_i}(q_{m_i}, \dot{q}_{m_i})\} \\ -\{\dot{Q}_i(t)J_{\Phi_i}^T(q_{m_i})M_b(q_b)J_{\Phi_i}(q_{m_i})\}\nu = 0 \end{aligned}$$

Property 2: The matrix $\dot{Q}_i(t)J_{\Phi_i}^T(q_{m_i})M_b(q_b)J_{\Phi_i}(q_{m_i})$ is bounded and uniformly continuous and meets the inequality [70]:

$$\| \dot{Q}_i(t)J_{\Phi_i}^T(q_{m_i})M_b(q_b)J_{\Phi_i}(q_{m_i}) \| \leq 2\eta, \forall t \geq 0, \tag{14}$$

where η is a positive constant.

Lemma 1: [58] Consider the continuous and differentiable bounded function $\phi(t)$, $\forall t \in [t_1, t_2]$, if $\phi(t)$ satisfies $\|\phi(t)\| \leq \iota$ where ι is a positive constant, then $\dot{\phi}(t)$ is bounded.

C. Radial Basis Function Neural Networks

Consider using RBFNNs to estimate a continuous function $\mathcal{F}(Z_i) : \mathbb{R}^\omega \to \mathbb{R}$ [68],

$$\mathcal{F}(Z_i) = W_i^{*T}S_i(Z_i) + \epsilon_i(Z_i),\ \forall Z_i \in \Omega_{Z_i} \tag{15}$$

where $W_i^* = [w_1, w_2, \ldots, w_h]^T \in \mathbb{R}^h$ is the ideal RBFNN weight vector, $h > 1$ is the node number of RBFNN, $Z_i = [z_1, z_2, \ldots, z_\omega]^T \in \Omega_Z \subset \mathbb{R}^\omega$ is the input vector, and $\epsilon_i(Z)$ is the bounded approximation error. Gaussian function is often selected as basis function

$$s_i(Z_i) = \exp[\frac{-(Z_i - \mu_i)^T(Z_i - \mu_i)}{\zeta_i^2}] \tag{16}$$

where $\mu_i = [\mu_{i1}, \mu_{i2}, \ldots, \mu_{i\omega}]^T$ is the center of given domain and ζ_i is the width of the Gaussian basis function. W_i^* is considered as W_i which minimizes $|\epsilon_i|$ for all Z_i

$$W_i^* = \arg\min_{W_i \in \mathbb{R}^h}\{\sup_{Z_i \in \Omega_{Z_i}} |\mathcal{F}_i(Z_i) - W_i^TS_i(Z_i)|\}. \tag{17}$$

III. Control Design

A. Model-Based Control Design

Defining $x_{1_i} = q_{m_i}$ and $x_{2_i} = \dot{q}_{m_i}$ and considering (13), we have the description of the cooperative dynamics as

$$\dot{x}_{1_i} = x_{2_i} \tag{18}$$

$$\begin{aligned} \dot{x}_{2_i} =& M_{c_i}^{-1}(x_{1_i})[Sat(\tau_i) + J_{\Phi_i}^T(x_{1_i})f_{I_i} - C_{c_i}(x_{1_i}, x_{2_i})x_{2_i} \\ &- G_{c_i}(x_{1_i}) - f_{dis_i}]. \end{aligned} \tag{19}$$

The position tacking error is expressed as $z_{1_i}(t) = x_{1_i}(t) - x_{d_i}(t)$ and $\dot{z}_{1_i}(t) = x_{2_i}(t) - \dot{x}_{d_i}(t)$. We lead into a virtual control $\alpha_{1_i}(t)$ and define a virtual error as $z_{2_i}(t) = x_{2_i}(t) - \alpha_{1_i}(t)$

$$\alpha_{1_i} = -K_{1_i}z_{1_i} + \dot{x}_{d_i} \tag{20}$$

where the gain matrix $K_{1_i} = K_{1_i}^T > 0$, and we have

$$\dot{z}_{1_i} = z_{2_i} + \alpha_{1_i} - \dot{x}_{d_i} = z_{2_i} - K_{1_i}z_{1_i}. \tag{21}$$

According to (21), differentiating z_{2_i} with respect to time, we have

$$\begin{aligned} \dot{z}_{2_i} =& M_{c_i}^{-1}(x_{1_i})[Sat(\tau_i) + J_{\Phi_i}^T(x_{1_i})f_{I_i} - C_{c_i}(x_{1_i}, x_{2_i})x_{2_i} \\ &- G_{c_i}(x_{1_i}) - f_{dis_i}] - \dot{\alpha}_{1_i}(t). \end{aligned} \tag{22}$$

The design of the disturbance observer consists of the following steps: 1) define a compounded disturbance, 2) define an auxiliary variable, 3) get the estimate of the auxiliary variable, 4) get the estimate of the disturbance.

We define a compounded function of disturbances as following

$$D_i(t) = \Delta\tau_i - f_{dis_i} \tag{23}$$

where the difference between the nominal input and the actual input is $\Delta\tau_i = Sat(\tau_i) - \tau_i$. Therefore, we can rewrite (22) as

$$\begin{aligned}\dot{z}_{2_i} =& M_{c_i}^{-1}(x_{1_i})[\tau_i + J_{\Phi_i}^T(x_{1_i})f_{I_i} - C_{c_i}(x_{1_i}, x_{2_i})x_{2_i} \\ &- G_{c_i}(x_{1_i}) + D_i(t)] - \dot{\alpha}_{1_i}(t)\end{aligned} \tag{24}$$

where $\| \dot{D}_i(t) \| \leq \beta$, and β is an unknown positive constant [58]. In order to design a nonlinear disturbance observer to estimate unknown variable $D_i(t)$, an auxiliary function is introduced as following:

$$z_{3_i} = D_i(t) - \Phi(z_{2_i}) \tag{25}$$

where a function vector $\Phi(z_{2_i})$ is to be proposed. According to (24) and (25), we have the derivative of z_{3_i} as

$$\begin{aligned}\dot{z}_{3_i} =& \dot{D}_i(t) - K_i(z_{2_i})\dot{z}_{2_i} \\ =& \dot{D}_i(t) + K_i(z_{2_i})\dot{\alpha}_{1_i}(t) - K_i(z_{2_i})M_{c_i}^{-1}(x_{1_i})[\tau_i \\ &+ J_{\Phi_i}^T(x_{1_i})f_{I_i} - C_{c_i}(x_{1_i}, x_{2_i})x_{2_i} - G_{c_i}(x_{1_i}) \\ &+ D_i(t)]\end{aligned} \tag{26}$$

where $K_i(z_{2_i}) = (\frac{\partial \Phi(z_{2_i})}{\partial z_{2_i}^T}) \in \mathbb{R}^{N_i \times N_i}$ is defined as the disturbance gain. For simplification and easy implementation, $\Phi(z_{2_i})$ is chosen as a linear function with respect to z_{2_i}. Then, we get that $K_i(z_{2_i})$ is a constant easily. For getting the estimate value of disturbance, we introduce the estimate value of $\dot{z}_{3_i}$ [60] as

$$\begin{aligned}\dot{\hat{z}}_{3_i} =& - K_i(z_{2_i})M_{c_i}^{-1}(x_{1_i})[\tau_i + J_{\Phi_i}^T(x_{1_i})f_{I_i} - C_{c_i}(x_{1_i}, x_{2_i})x_{2_i} \\ &- G_{c_i}(x_{1_i}) + \hat{D}_i(t)] + K_i(z_{2_i})\dot{\alpha}_{1_i}(t).\end{aligned} \tag{27}$$

According to (25), we can have the estimate of disturbance $D_i(t)$ as

$$\hat{D}_i(t) = \hat{z}_{3_i} + \Phi(z_{2_i}). \tag{28}$$

And it is easy to get

$$\tilde{z}_{3_i} = \hat{z}_{3_i} - z_{3_i} = \hat{D}_i(t) - D_i(t) = \tilde{D}_i(t). \tag{29}$$

Differentiating $\tilde{D}_i(t)$ with respect to time and considering (26) and (27), we obtain

$$\begin{aligned}\dot{\tilde{D}}_i(t) = \dot{\tilde{z}}_{3_i} =& \dot{\hat{z}}_{3_i} - \dot{z}_{3_i} \\ =& - \dot{D}_i(t) - K_i(z_{2_i})M_{c_i}^{-1}(x_{1_i})\tilde{D}_i(t).\end{aligned} \tag{30}$$

When $M_{c_i}(x_{1_i})$, $C_{c_i}(x_{1_i}, x_{2_i})$, $G_{c_i}(x_{1_i})$, and $J_{\Phi_i}^T(x_{1_i})f_{I_i}$ are known, we propose the model-based control as

$$\begin{aligned}\tau_i =& - z_{1_i} - K_{2_i}z_{2_i} - J_{\Phi_i}^T(x_{1_i})f_{I_i} - \hat{D}_i(t) + G_{c_i}(x_{1_i}) \\ &+ C_{c_i}(x_{1_i}, x_{2_i})\alpha_{1_i}(t) + M_{c_i}(x_{1_i})\dot{\alpha}_{1_i}(t).\end{aligned} \tag{31}$$

where the gain matrix $K_{2_i} = K_{2_i}^T > 0$.

Theorem 1: For the dynamic of CMM described by (13), the controller (31) guarantees that z_{1_i}, z_{2_i} and $\tilde{D}_i(t)$ are semi-globally uniformly bounded. The tracking error z_{1_i} will converge to the compact sets $\Omega_{z_{1_i}} := \{z_{1_i} \epsilon R^{N_i} |\ ||z_{1_i}|| \leq \sqrt{O_1}\}$ where $O_1 = 2(V_2(0) + C_1)/\rho_{1_i}$. ρ_1 and C_1 are two positive constants.

Proof: We consider a Lyapunov function candidate as

$$V_{1_i} = \frac{1}{2}z_{1_i}^T z_{1_i} \tag{32}$$

and taking its time derivative, we have

$$\dot{V}_{1_i} = -z_{1_i}^T K_{1_i} z_{1_i} + z_{1_i}^T z_{2_i}. \tag{33}$$

Then we have the Lyapunov function candidate as

$$V_{2_i} = V_{1_i} + \frac{1}{2}z_{2_i}^T M_{c_i}(x_{1_i})z_{2_i} + \frac{1}{2}\tilde{D}_i^T(t)\tilde{D}_i(t). \tag{34}$$

Combining (24) and (33) and differentiating (34) with respect to time yields

$$\begin{aligned}\dot{V}_{2_i} =& - z_{1_i}^T K_{1_i} z_{1_i} + z_{1_i}^T z_{2_i} + \frac{1}{2}z_{2_i}^T \dot{M}_{c_i}(x_{1_i})z_{2_i} + z_{2_i}^T[\tau_i \\ &+ J_{\Phi_i}^T(x_{1_i})f_{I_i} - C_{c_i}(x_{1_i}, x_{2_i})x_{2_i} - G_{c_i}(x_{1_i}) + D_i(t) \\ &- M_{c_i}(x_{1_i})\dot{\alpha}_{1_i}(t)] + \tilde{D}_i(t)^T \dot{\tilde{D}}_i(t).\end{aligned} \tag{35}$$

we know that $\frac{1}{2}z_{2_i}^T\{\dot{M}_{c_i}(q_{m_i}) - 2C_{c_i}(q_{m_i}, \dot{q}_{m_i})\}z_{2_i} = \frac{1}{2}z_{2_i}^T\{\dot{Q}_i(t)J_{\Phi_i}^T(q_{m_i})M_b(q_b)J_{\Phi_i}(q_{m_i})\}z_{2_i}$ and substituting it into (35) leads to

$$\begin{aligned}\dot{V}_{2_i} =& - z_{1_i}^T K_{1_i} z_{1_i} + z_{1_i}^T z_{2_i} + \frac{1}{2}z_{2_i}^T \dot{Q}_i(t)J_{\Phi_i}^T(q_{m_i})M_b(q_b) \\ &\times J_{\Phi_i}(q_{m_i})z_{2_i} + z_{2_i}^T[\tau_i + J_{\Phi_i}^T(x_{1_i})f_{I_i} \\ &- C_{c_i}(x_{1_i}, x_{2_i})\alpha_{1_i} - G_{c_i}(x_{1_i}) + D_i(t) \\ &- M_{c_i}(x_{1_i})\dot{\alpha}_{1_i}(t)] + \tilde{D}_i^T(t)\dot{\tilde{D}}_i(t).\end{aligned} \tag{36}$$

Because of $\| \dot{Q}_i(t)J_{\Phi_i}^T(q_{m_i})M_b(q_b)J_{\Phi_i}(q_{m_i}) \| \leq 2\eta$, $\forall t \geq 0$, where η is a positive constant, thus we can get

$$\begin{aligned}\dot{V}_{2_i} \leq& - z_{1_i}^T K_{1_i} z_{1_i} + z_{1_i}^T z_{2_i} + \eta z_{2_i}^T z_{2_i} + z_{2_i}^T[\tau_i + J_{\Phi_i}^T(x_{1_i})f_{I_i} \\ &- C_{c_i}(x_{1_i}, x_{2_i})\alpha_{1_i} - G_{c_i}(x_{1_i}) + D_i(t) \\ &- M_{c_i}(x_{1_i})\dot{\alpha}_{1_i}(t)] + \tilde{D}_i^T(t)[-\dot{D}_i(t) \\ &- K_i(z_{2_i})M_{c_i}^{-1}(x_{1_i})\tilde{D}_i(t)].\end{aligned} \tag{37}$$

Substituting (31) into (37), we have

$$\begin{aligned}\dot{V}_{2_i} \leq& - z_{1_i}^T K_{1_i} z_{1_i} - z_{2_i}^T(K_{2_i} - \eta I - \frac{1}{2}I)z_{2_i} - \tilde{D}_i^T(t) \\ &\times (K_i(z_{2_i})M_{c_i}^{-1}(x_{1_i}) - I)\tilde{D}_i(t) + \frac{1}{2} \| \dot{D}_i(t) \|^2 \\ &\leq -\rho_{1_i}V_{2_i} + C_{1_i}.\end{aligned} \tag{38}$$

where

$$\begin{aligned}\rho_{1_i} =& \min\big(2\lambda_{\min}(K_{1_i}), \frac{2\lambda_{\min}(K_{2_i} - \eta I - \frac{1}{2}I)}{\lambda_{\max}(M_{c_i}(x_{1_i}))}, \\ & 2\lambda_{\min}(K_i(z_{2_i})M_{c_i}^{-1}(x_{1_i}) - I)\big), \\ C_{1_i} =& \frac{1}{2}\beta^2\end{aligned} \tag{39}$$

with $\lambda_{\min}(\bullet)$ and $\lambda_{\max}(\bullet)$ defined as the minimum and maximum eigenvalues of matrix $\bullet$, respectively. For ensuring

$\rho_{1_i} > 0$, the system parameters must be chosen to satisfy the following conditions:

$$\lambda_{\min}(K_{1_i}) > 0, \lambda_{\min}(K_{2_i} - \eta I - \frac{1}{2}I) > 0,$$
$$\lambda_{\min}(K_i(z_{2_i})M_{c_i}^{-1}(x_{1_i}) - I) > 0. \tag{40}$$

Then, considering the Lyapunov function candidate $V_2 = \sum_{i=1}^{r} V_{2_i}$ and the property of the internal forces, we can get

$$\begin{aligned}\dot{V}_2 \leq& -\sum_{i=1}^{r} \rho_{1_i} V_{2_i} + \sum_{i=1}^{r} C_{1_i}\\ \leq& -\rho_1 V_2 + C_1\end{aligned} \tag{41}$$

where $\rho_1 = \min_{1\leq i\leq r}(\rho_{1_i})$, $C_1 = \sum_{i=1}^{r} C_{1_i}$.

From the above analysis, it is straightforward to show that the signals z_{1_i}, z_{2_i} and $\tilde{D}_i(t)$ are semiglobally uniformly bounded. Thus, according to the boundedness of x_{d_i}, we can consider that x_{1_i} is bounded. Since $\dot{x}_{d_i}$ is bounded as well and α_{1_i} is bounded, x_{2_i} is bounded, too. For completeness, the details of the proof are provided here.

Multiplying (41) by $e^{\rho_1 t}$ yields

$$\frac{d}{dt}(V_2 e^{\rho_1 t}) \leq C_1 e^{\rho_1 t}. \tag{42}$$

Integrating above the inequality, we have

$$V_2 \leq \Big(V_2(0) - \frac{C_1}{\rho_1}\Big)e^{-\rho_1 t} + \frac{C_1}{\rho_1} \leq V_2(0) + \frac{C_1}{\rho_1}. \tag{43}$$

Then, because $V_2 = \sum_{i=1}^{r} V_{2_i}$, $V_{2_i} \leq V_2$, we have

$$\frac{1}{2} \parallel z_{1_i} \parallel^2 \leq V_2(0) + \frac{C_1}{\rho_1} = \frac{1}{2}O_1. \tag{44}$$

Therefore, z_{1_i} converges to a small range $\Omega_{z_{1_i}}$. Bounds for z_{2_i} and $\tilde{D}_i(t)$ can be proved similarly and what we presented above is the conclusion of *Proof.*

B. Adaptive Neural Network Control Design

Since uncertainties exist in $M_{c_i}(x_{1_i})$, $C_{c_i}(x_{1_i}, x_{2_i})$, $G_{c_i}(x_{1_i})$, $J_{\Phi_i}^T(x_{1_i})f_{I_i}$, the model-based control design may not be realizable because of uncertainties. To overcome these challenges, a controller based on RBFNN is utilized to approximate the uncertainties and improve the performance of the system via the online estimation. For using this method, we need to divide the actual value $M_{c_i}(x_{1_i})$ into two parts. One is the virtual part which we denote as $M_{v_i}(x_{1_i})$, the other is the uncertain part represented as $\Delta M_i(x_{1_i}) = M_{c_i}(x_{1_i}) - M_{v_i}(x_{1_i})$. Similarly, we choose the virtual part $C_{v_i}(x_{1_i}, x_{2_i})$ so that $\dot{M}_{v_i}(x_{1_i}) - 2C_{v_i}(x_{1_i}, x_{2_i})$ is skew symmetric and $\Delta C_i(x_{1_i}, x_{2_i}) = C_{c_i}(x_{1_i}, x_{2_i}) - C_{v_i}(x_{1_i}, x_{2_i})$. We propose the controller as follows

$$\begin{aligned}\tau_i =& -z_{1_i} - K_{2_i}z_{2_i} - \hat{D}_i(t) + C_{v_i}(x_{1_i}, x_{2_i})\alpha_{1_i}\\ &+ \hat{W}_i^T S_i(Z_i)\end{aligned} \tag{45}$$

where $\hat{W}_i$ is the weight of RBFNN and $S_i(Z_i)$ is the basis function of RBFNN. $\hat{W}_i^T S(Z_i)$ is used to estimate $W_i^{*T} S_i(Z_i)$ and $W_i^{*T} S_i(Z_i)$ is defined as

$$\begin{aligned}W_i^{*T} S_i(Z_i) =& \Delta C_{c_i}(x_{1_i}, x_{2_i})x_{2_i} + \Delta M_{c_i}(x_{1_i})\dot{z}_{2_i}\\ &+ M_{c_i}(x_{1_i})\dot{\alpha}_{1_i} - J_{\Phi_i}^T(x_{1_i})f_{I_i} + G_{c_i}(x_{1_i})\\ &- \epsilon_i(Z_i)\end{aligned} \tag{46}$$

where $Z_i = [x_{1_i}, x_{2_i}, \dot{z}_{2_i}, \dot{\alpha}_{1_i}]^T$ is the input variable of RBFNN and $\epsilon_i(Z_i)$ is the approximation error of RBFNN. The adaptive law is proposed as

$$\dot{\hat{W}}_i = -\Gamma_i[S_i(Z_i)z_{2_i} + \sigma_i \hat{W}_{j,i}] \tag{47}$$

where Γ_i is a constant gain matrix and $\sigma_i > 0$ is a small positive constant. Therefore, on the basis of (46), (24) is redefined as follows

$$\begin{aligned}M_{v_i}(x_{1_i})\dot{z}_{2_i} =& \tau_i - C_{v_i}(x_{1_i}, x_{2_i})x_{2_i} - W_i^{*T} S_i(Z_i)\\ &- \epsilon_i(Z_i) + D_i(t).\end{aligned} \tag{48}$$

The auxiliary function is the same as one of the model-based control. Similarly, it can be obtained that

$$\begin{aligned}\dot{z}_{3_i} =& \dot{D}_i(t) - K_i(z_{2_i})\dot{z}_{2_i}\\ =& \dot{D}_i(t) - K_i(z_{2_i})M_{v_i}^{-1}(x_{1_i})[\tau_i - C_{v_i}(x_{1_i}, x_{2_i})x_{2_i}\\ &- W_i^{*T} S_i(Z_i) - \epsilon_i(Z_i) + D_i(t)].\end{aligned} \tag{49}$$

For getting the estimate value of disturbances, the estimate value of $\dot{z}_{3_i}$ is given as

$$\begin{aligned}\dot{\hat{z}}_{3_i} =& -K_i(z_{2_i})M_{v_i}^{-1}(x_{1_i})(\tau_i - C_{v_i}(x_{1_i}, x_{2_i})x_{2_i}\\ &+ \hat{D}_i(t)).\end{aligned} \tag{50}$$

Thus, it is easy to get that

$$\tilde{z}_{3_i} = \hat{z}_{3_i} - z_{3_i} = \hat{D}_i(t) - D_i(t) = \tilde{D}_i(t). \tag{51}$$

According to (49) and (50), differentiating $\tilde{D}_i(t)$ with respect to time, it is got that

$$\begin{aligned}\dot{\tilde{D}}_i(t) =& -\dot{D}_i(t) - K_i(z_{2_i})M_{v_i}^{-1}(x_{1_i})[W_i^{*T} S_i(Z_i)\\ &+ \epsilon_i(Z_i) + \tilde{D}_i(t)].\end{aligned} \tag{52}$$

Theorem 2: For the dynamic of CMM described by (13), the controller (45) with the adaptive law (47) guarantees that z_{1_i}, z_{2_i}, $\tilde{D}_i(t)$, $\tilde{W}_i$ are semi-globally uniformly bounded. The error signals z_{1_i} will converge to the compact sets $\Omega_{z_{1_i}} := \{z_{1_i} \epsilon R^{N_i} |\ ||z_{1_i}|| \leq \sqrt{O_2}\}$ where $O_2 = 2(V_3(0) + C_2/\rho_2)$. ρ_2 and C_2 are two positive constants.

Proof: the Lyapunov function is proposed by us as

$$\begin{aligned}V_{3_i} =& \frac{1}{2}z_{1_i}^T z_{1_i} + \frac{1}{2}z_{2_i}^T M_{v_i}(x_{1_i})z_{2_i} + \frac{1}{2}\tilde{D}_i^T(t)\tilde{D}_i(t)\\ &+ \frac{1}{2}\sum_{j=1}^{n} \tilde{W}_{j,i}^T \Gamma_i^{-1} \tilde{W}_{j,i}\end{aligned} \tag{53}$$

where $\tilde{W}_{j,i} = \hat{W}_{j,i} - W_{j,i}^*$, and $\tilde{W}_{j,i}$, $\hat{W}_{j,i}$ and $W_{j,i}^*$ are the RBFNN weight error, estimate and actual value, respectively. Differenting V_{3_i} with respect to time and substituting (48) into

$\dot{V}_{3_i}$, we can get

$$\begin{aligned}\dot{V}_{3_i} \le & -z_{1_i}^T K_{1_i} z_{1_i} + z_{1_i}^T z_{2_i} + z_{2_i}^T[\tau_i - C_{v_i}(x_{1_i}, x_{2_i})\alpha_{1_i} \\ & - W_i^{*T} S_i(Z) - \epsilon_i(Z_i) + D_i(t)] + \tilde{D}_i^T(t)\dot{\tilde{D}}_i(t) \\ & + \sum_{j=1}^{n} \tilde{W}_{j,i}^T \Gamma_i^{-1} \dot{\hat{W}}_i. \end{aligned} \tag{54}$$

Then, substituting the controller (45), adaptive law (47) and (52) into (54), we can obtain

$$\begin{aligned}\dot{V}_{3_i} \le & -z_{1_i}^T K_{1_i} z_{1_i} - z_{2_i}^T K_{2_i} z_{2_i} - z_{2_i}^T \tilde{D}_i(t) - \tilde{D}_i^T(t)\dot{D}_i(t) \\ & - \tilde{D}_i^T(t) K_i(z_{2_i}) M_{v_i}^{-1}(x_{1_i})[W_i^{*T} S_i(Z_i) + \epsilon_i(Z_i) \\ & + \tilde{D}_i(t)] - z_{2_i}^T \epsilon_i(Z_i) - \sum_{j=1}^{n} \tilde{W}_{j,i}^T \sigma_i \hat{W}_{j,i} \end{aligned} \tag{55}$$

Applying the Young's inequality, it will be easy to get

$$-\sum_{j=1}^{n} \tilde{W}_{j,i}^T \sigma_i \hat{W}_{j,i} \le \sum_{j=1}^{n} \frac{\sigma_i}{2}(\| W_{j,i}^* \|^2 - \| \tilde{W}_{j,i} \|^2). \tag{56}$$

Further, subistituting (56) into (55), we obtain

$$\begin{aligned}\dot{V}_{3_i} \le & -z_{1_i}^T K_{1_i} z_{1_i} - z_{2_i}^T (K_{2_i} - I) z_{2_i} + \| \epsilon(Z_i) \|^2 + \frac{1}{2}\beta^2 \\ & - \tilde{D}_i^T(t)[K_i(z_{2_i}) M_{v_i}^{-1}(x_{1_i}) - (\| K_i(z_{2_i}) M_b^{-1}(x_{1_i}) \|^2 \\ & + 1)I]\tilde{D}_i(t) + \sum_{j=1}^{n} \frac{\sigma_i + \| S_{j,i}(Z_i) \|^2}{2} \| W_{j,i}^* \|^2 \\ & - \sum_{j=1}^{n} \frac{\sigma_i}{2} \| \tilde{W}_{j,i} \|^2 . \end{aligned} \tag{57}$$

And because we have $\| S_{j,i}(Z) \| \le s_j$, where the joint number $j = 1, 2, \ldots, n$, $s_j > 0$ [72]. $\dot{V}_{3_i}$ is shown as follow

$$\begin{aligned}\dot{V}_{3_i} \le & -z_{1_i}^T K_{1_i} z_{1_i} - z_{2_i}^T (K_{2_i} - I) z_{2_i} + \| \epsilon_i(Z_i) \|^2 \\ & - \tilde{D}_i^T(t)[K_i(z_{2_i}) M_{v_i}^{-1}(x_{1_i}) - (\| K_i(z_{2_i}) \\ & \times M_b^{-1}(x_{1_i}) \|^2 + 1)I]\tilde{D}_i(t) + \frac{1}{2}\beta^2 \\ & + \sum_{j=1}^{n} \frac{\sigma_i + s_j^2}{2} \| W_{j,i}^* \|^2 - \sum_{j=1}^{n} \frac{\sigma_i}{2} \| \tilde{W}_{j,i} \|^2 \\ & \le -\rho_{2_i} V_{3_i} + C_{2_i} \end{aligned} \tag{58}$$

where

$$\begin{aligned}\rho_{2_i} = & \min\big(2\lambda_{\min}(K_{1_i}), \frac{2\lambda_{\min}(K_{2_i} - I)}{\lambda_{\max}(M_{c_i}(x_{1_i}))}, 2\lambda_{\min}(K_i(z_{2_i}) \\ & \times M_{v_i}^{-1}(x_{1_i}) - (\| K_i(z_{2_i}) M_{v_i}^{-1}(x_{1_i}) \|^2 + 1)I), \\ & \min(\frac{\sigma_i}{\lambda_{\max}(\Gamma_i^{-1})})\big) \\ C_{2_i} = & \| \epsilon_i(Z_i) \|^2 + \frac{1}{2}\beta^2 + \sum_{i=1}^{n} \frac{\sigma_i + s_i^2}{2} \| W_i^* \|^2 . \end{aligned} \tag{59}$$

Then, considering the Lyapunov function candidate $V_3 = \sum_{i=1}^{r} V_{3_i}$ and the property of the internal forces, we can get

$$\begin{aligned}\dot{V}_3 \le & -\sum_{i=1}^{r} \rho_{2_i} V_{3_i} + \sum_{i=1}^{r} C_{2_i} \\ \le & -\rho_2 V_3 + C_2 \end{aligned} \tag{60}$$

where $\rho_2 = \min_{1 \le i \le r}(\rho_{2_i})$, $C_2 = \sum_{i=1}^{r} C_{2_i}$.

To ensure the closed-loop system stability, we have $\rho_2 > 0$. So the control parameters are chosen to satisfy the following conditions:

$$\begin{aligned}& \lambda_{\min}(K_{1_i}) > 0, \lambda_{\min}(K_{2_i} - I) > 0, \\ & \lambda_{\min}(K_i(z_{2_i}) M_{v_i}^{-1}(x_{1_i}) - (\| K_i(z_{2_i}) M_{v_i}^{-1}(x_{1_i}) \|^2 \\ & + 1)I) > 0, \lambda_{\min}(\sigma_i) > 0. \end{aligned} \tag{61}$$

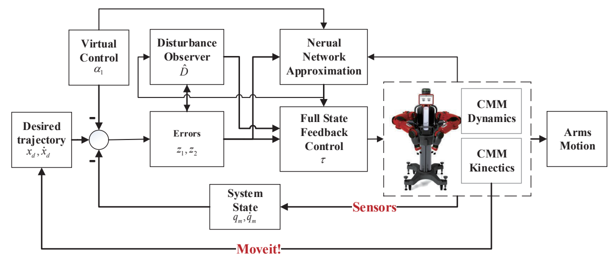

Fig. 2: Full state feedback strategy of CMM.

From the above analysis and the proof of Theorem 1, $||z_{1_i}|| \le \sqrt{O_2}$. z_{1_i} converges to a small range $\Omega_{z_{1_i}}$. z_{1_i}, z_{2_i} and $\tilde{D}_i(t)$ can be proved to be similarly semiglobally uniformly bounded. z_{1_i}, z_{2_i} and $\tilde{D}_i(t)$ can converge to $\Omega_{z_{1_i}}$, $\Omega_{z_{2_i}}$, and $\Omega_{\tilde{D}_i}$. Because W_i^* are constants, we know that $\hat{W}_i$ are also bounded. The full state feedback control strategy is shown in Fig. 2.

IV. EXPERIMENTS

In this paper, a humanoid vertical 7-joint robot (Baxter) based on ROS (Robotic Operating System) is utilized to build a robot motion control platform. ROS is a robot development environment integrating a variety of robot hardware drivers, some common robot function modules, a unified programming, compilation, and debugging environment. The proposed Baxter robot control system consists of a master computer, a slave computer, an embedded controller, drivers, and a grabbed object.

Theoretical analysis has demonstrated that the proposed RBFNN controller has a good control effect. Then we applied the controller on the dual-arm cooperative robot (Baxter) manufactured by Rethink Robotics and checked whether the RBFNN controller can also get better results than the PID controller in the real environment. We designed an experiment to let the Baxter robot to hold a small basketball with dual arms and move along a straight line under the proposed controller, which was demonstrated in Fig. 3. That is, seven degrees of freedom of the robot arm need to be controlled by the proposed RBFNN control. In addition, a general PID controller is used to achieve the same function. By observing the experimental results of two different controllers, the theoretical derivation is verified.

In this set of experiments, we used two computers to process the data. One computer was used as the master controller (connecting Baxter robots and slave controllers, controlling the Baxter robot directly and transferring data from the controllers and equipped with Linux operating system). Another computer acted as the slave controller (connecting the master controller, efficiently processing data and assisting control, equipped with Windows operating system). The entire control system communication and components are shown in Fig. 4. Spline interpolation is an interpolation method that is commonly used in industrial design to obtain a smooth curve, and cubic spline is a more widely used one. The path planning of the robotic arm was finished by ROS MoveIt. A set of hundred pairs of joint angles and their corresponding times were collected and the cubic spline interpolation algorithm was used to interpolate the acquired data. Through cubic spline interpolation, we were able to get the planned joint trajectory, velocity and acceleration.

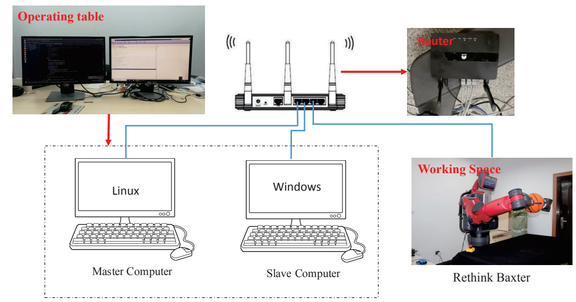

Fig. 4: The entire control system communication and components.

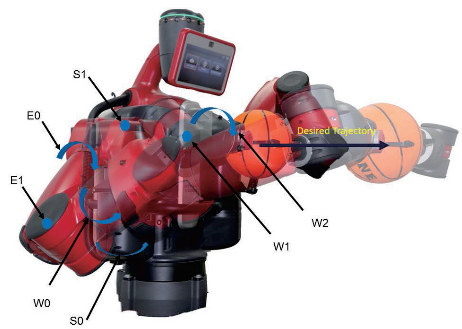

Fig. 3: The demonstration of Baxter experimental results.

Due to the limited computing speed of computers, a master computer and a slave computer were were connected to each other via Ethernet. The transmission frequency and the receiving frequency of master computer were set to real-time and 200Hz, respectively. The full closed-loop servo frequency was set to 250Hz. In order to obtain more considerable experimental contrasts, we set the same initial conditions for the verification of both controllers. Under the initial conditions, the small basketball was held by both arms from the beginning. A decentralized adaptive RBFNN control combined with disturbance observers is proposed to deal with the unknown actuator input saturations in the dual arm robot system.

TABLE I: PARAMETERS USED FOR PID EXPERIMENT

Joints \ PARM	left arm			right arm		
	K_P	K_I	K_D	K_P	K_I	K_D
S0	35.0	4.0	4.0	17.7	0.01	3.1
S1	15.0	2.0	4.0	15.0	6.0	3.0
E0	14.0	0.2	3.0	18.0	1.5	3.1
E1	25.0	0.2	3.0	20.0	1.5	3.5
W0	50.0	0.2	2.5	18.7	1.0	5.2
W1	60.0	0.2	1.3	26.0	1.2	5.2
W2	5.1	0.1	2.5	10.3	0.1	2.1

1) PID Control: In this section, a common PID controller was used to control seven joints of the Baxter robot [73], [74], so that the pose of the end-effector performed the desired trajectory planning. Table I illustrated the PID parameters corresponding to the seven joints of the left and right arms, respectively. For joints (S0, S1, E0, E1, W0, W1 and W2), PID parameters corresponded to K_P, K_I, K_D.

The left and right two-arm experimental results of the PID controller are shown in Fig. 5 and Fig. 6, respectively, where the red, green and blue lines represent the actual, expected and error values, respectively. Observing the experimental results of the two arms, it can be obtained that the actual value of the PID control can roughly follow the change of the expected value, and the error value of most joints is also within a reasonable range.

However, some joints still have large error values. The tracking error exceeds 0.08 rad in some time segments. It can be seen from Fig. 5(h) and Fig. 6(h) that the position tracking of the end effector is not very satisfactory. In actual applications, accurate positions of joints cannot be guaranteed. At the same time, we can see from Fig. 7 that the left arm has considerable torque fluctuations at E1 and S1 and the right arm has considerable torque fluctuations at W2 and E1 under the constraint of input saturation while others do not have. Each joint of the Baxter robot has a peak torque specification which is the maximum amount of torque that should be demanded from (or experienced by) each joint. These are shown in Table II. However, if the object being handled results in higher torque levels, the actuators will saturate, resulting in additional nonlinearities.

TABLE II: Peak Joint Torque Specifications of Baxter Joints (Source: https://sdk.rethinkrobotics.com/wiki/Hardware_Specifications)

Joint	Peak Torque
S0, S1, E0, E1	50Nm
W0, W1, W2	15Nm

It is argued in this article that the proposed controller can still achieve satisfied trajectory control despite saturation. However, for the experimental evaluations, rather than designing an experiment that requires higher torque levels than those specified in Table II, virtual saturation values of 2.0 Nm are set for each joint. In this way, possible damage to Baxter will be avoided.

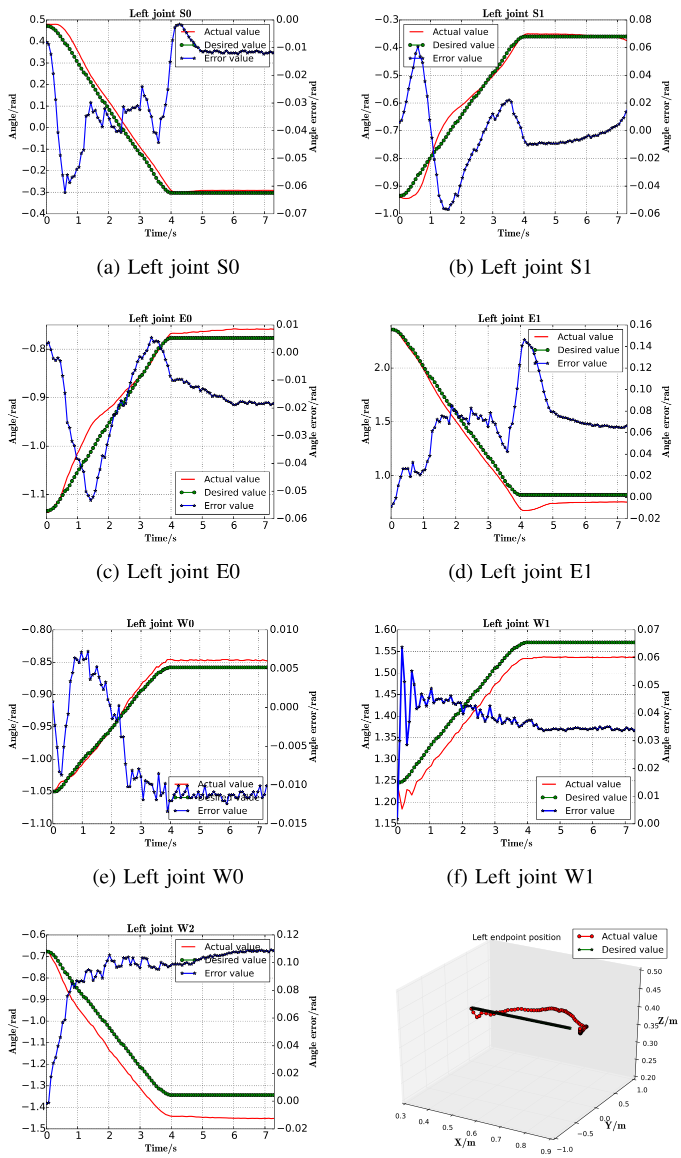

(a) Left joint S0 (b) Left joint S1 (c) Left joint E0 (d) Left joint E1 (e) Left joint W0 (f) Left joint W1 (g) Left joint W2 (h) Left endpoint position

Fig. 5: The experimental results for the seven joints of the left arm under PID control.

The torque value obtained by the PID controller is relatively large and it is easy to achieve input saturation. Therefore, a better control method needs to be sought. In addition to image contrast, the mean square error (MSE) was used to compare controllers. It is defined as follows:

$$E_c(k) = \frac{1}{n}\sum_{k=1}^{n}[Y_d(k) - Y_p(k)]^2 \tag{62}$$

where $Y_d(k)$ and $Y_p(k)$ denotes output of desired and actual plant. [75]–[77].

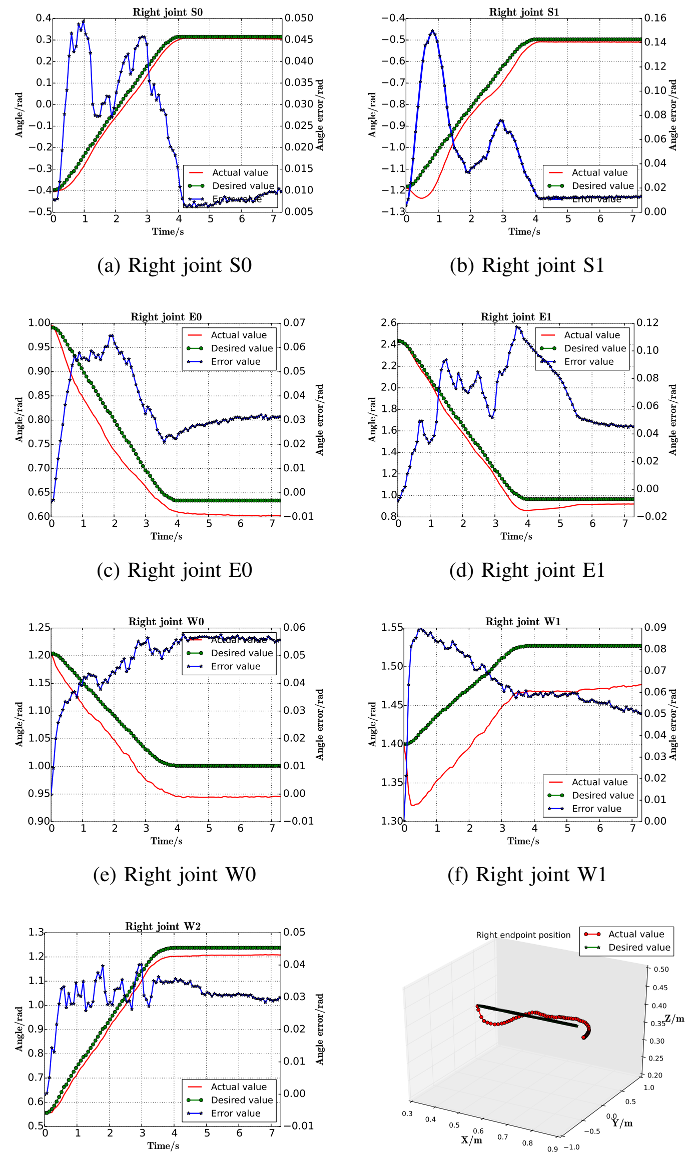

(a) Right joint S0 (b) Right joint S1 (c) Right joint E0 (d) Right joint E1 (e) Right joint W0 (f) Right joint W1 (g) Right joint W2 (h) Right endpoint position

Fig. 6: The experimental results for the seven joints of the right arm under PID control.

TABLE III: PARAMETERS USED FOR RBFNN EXPERIMENT

PARM / Joints	left arm		right arm	
	K_1	K_2	K_1	K_2
S0	20.6	12.1	17.7	5.1
S1	20.0	8.5	15	18
E0	22.0	4.0	18.0	4.1
E1	20.3	5.1	22.0	4.5
W0	17.7	3.1	16.7	4.2
W1	30.0	2.8	26.0	3.5
W2	15.7	4.2	10.3	2.1

2) Neural Network Cooperative Control Based on Disturbance Observer: There are seven groups of RBFNN parameters, which match the seven joints of Baxter's left limb and right limb. In the theoretical part, we proposed the RBFNN dual-arm cooperative controller with disturbance observers and considered the input saturation problem, and verified it by using the Lyapunov method. In this part, we applied the proposed controller on Baxter to verify the controller. For its control effect, we used ROS MoveIt to plan the trajectory for all joints of the arms, and then obtained the expected values for each joint.

Next, we used the cubic spline difference algorithm to obtain smooth position and velocity expectations. Through experiments, we obtained the left and right arm controller gains K_1 and K_2 as shown in Table III.

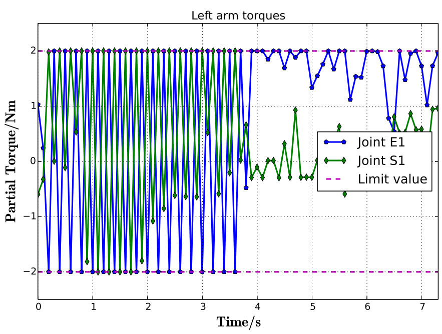

(a) Left arm torques

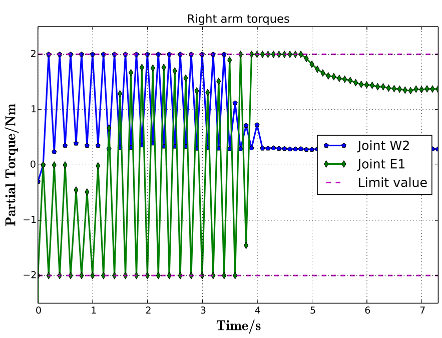

(b) Right arm torques

Fig. 7: The input torques for the dual arms under PID control.

As for the gains of the RBFNN, σ is chosen as $\sigma = 0.002$, the number of RBFNN nodes are 7^3, and the adaptive gain matrix is chosen as a diagonal matrix $\Gamma = 500 I_{Node}$, where $Node = 7^3$. The disturbance gain is chosen as 19.5. The control performance of the proposed controller (45) is shown in Fig. 8 and Fig. 9, in which the red, green and blue lines respectively represent the actual value, the expected value, and the error value. From the perspective of the joint angle tracking, under the action of the controller, it can be seen that the actual value of the joint can follow the expected joint value well, and the joint error value is constrained to a small zero field. From Fig. 8(h) and Fig. 9(h), it can be seen that the position of the end effector is basically consistent with the desired trajectory, and a good control effect is achieved during the grasping. From Fig. 10, it can be also seen that the joint torque variation is not too large and does not reach the peak torque of the joint.

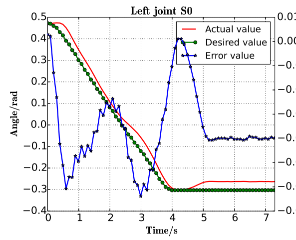

(a) Left joint S_0

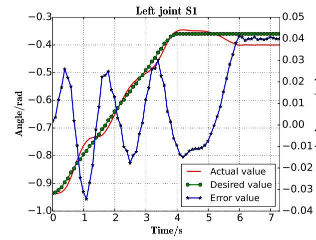

(b) Left joint S_1

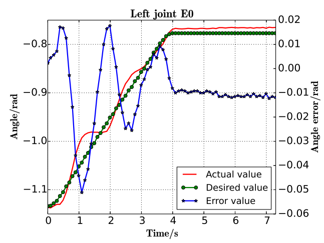

(c) Left joint E_0

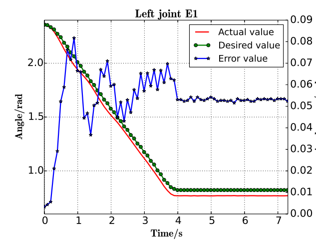

(d) Left joint E_1

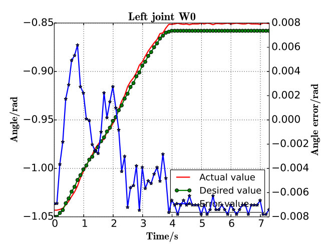

(e) Left joint W_0

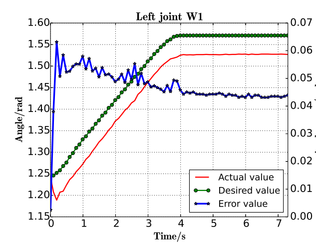

(f) Left joint W_1

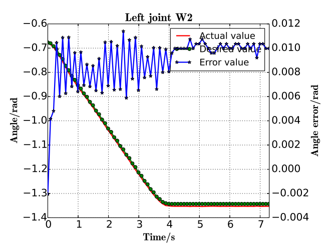

(g) Left joint W_2

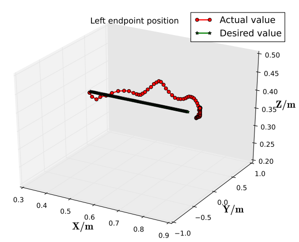

(h) Left endpoint position

Fig. 8: The experimental results for the seven joints of the left arm under RBFNN control.

A. The Conclusion of Experiments

Through the analysis of the above two experimental results, it can be concluded that compared with the PID controller, robotic systems under RBFNN controller showed better tracking performances in the joint and task space. The joint torque also has a better performance. The proposed controller results in a more accurate control and compensates for the errors caused by the unknown model and external disturbances of the Baxter robot during operation. Furthermore, the average MSE obtained with different control methods when the control program is run for 100 iterations are shown in Table IV. From the table, it can be seen that average MSE obtained with proposed RBFNN controller is smaller when compared to MSE obtained when the PID controller is used.

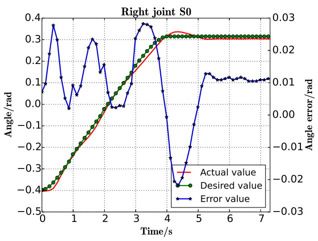

(a) Right joint S_0

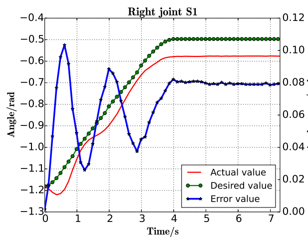

(b) Right joint S_1

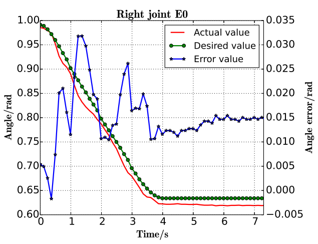

(c) Right joint E_0

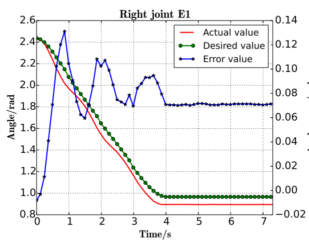

(d) Right joint E_1

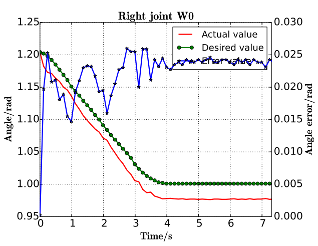

(e) Right joint W_0

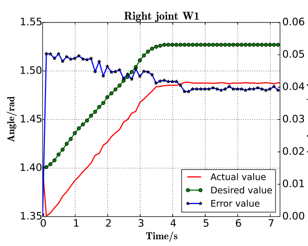

(f) Right joint W_1

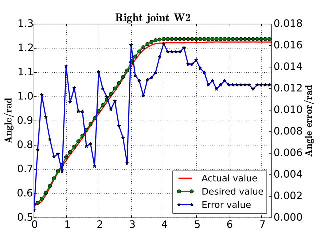

(g) Right joint W_2

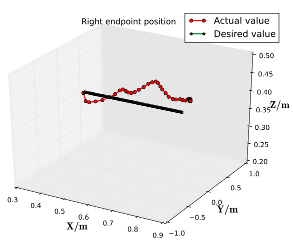

(h) Right endpoint position

Fig. 9: The experimental results for the seven joints of the right arm under RBFNN control.

TABLE IV: Average MSE(m) obtained during the online control (after 100 iterations)

Joints \ controller	left arm		right arm	
	RBFNN	PID	RBFNN	PID
S0	0.00029483	0.00970988	0.05624237	0.00112485
S1	0.00018958	0.01251787	0.00122080	0.04465377
E0	0.00018969	0.00333228	0.00323846	0.01046209
E1	0.00836467	0.10418332	0.00835309	0.02018356
W0	0.00024106	0.00116844	0.00586101	0.00738964
W1	0.01180708	0.02355597	0.00800097	0.02730591
W2	0.00016269	0.01787146	0.00400777	0.00290976

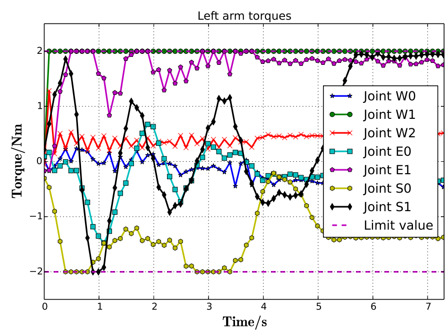

(a) Left arm torques

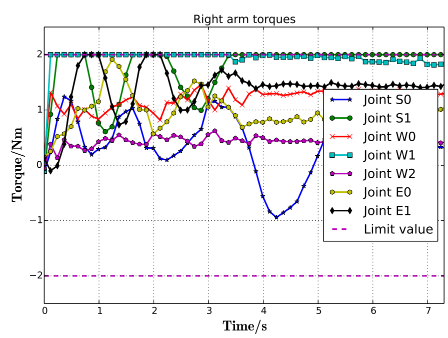

(b) Right arm torques

Fig. 10: The input torques for the dual arms under RBFNN cooperative control.

V. Conclusion

In this paper, the state feedback controllers that combine RBFNN approximation and disturbance observers are developed to alleviate the problems of the unknown dynamic model of coordinated multiple robotic manipulators under the influence of unknown disturbances. Simultaneously, an adaptive RBFNN controller is used to deal with the problem of the saturation nonlinearity of the motor. Through the Lyapunov stability analysis and experiments, the proposed controller is proven to achieve semi-globally uniformly boundedness.

References

[1] H.-S. Kim and J.-B. Song, "Multi-dof counterbalance mechanism for a service robot arm," *IEEE/ASME Transactions on Mechatronics*, vol. 19, no. 6, pp. 1756–1763, 2014.

[2] Y. Cai, Z. Tang, Y. Ding, and B. Qian, "Theory and application of multi-robot service-oriented architecture," *IEEE/CAA Journal of Automatica Sinica*, vol. 3, no. 1, pp. 15–25, 2016.

[3] Y. Li and S. S. Ge, "Human–robot collaboration based on motion intention estimation," *IEEE/ASME Transactions on Mechatronics*, vol. 19, no. 3, pp. 1007–1014, 2014.

[4] G. Wu, J. Sun, and J. Chen, "Optimal linear quadratic regulator of switched systems," *IEEE Transactions on Automatic Control*, 2018, to be published, DOI: 10.1109/TAC.2018.2872204.

[5] X. Ning, Y. Yang, Z. Li, M. Gui, and J. Fang, "Ephemeris corrections in celestial/pulsar navigation using time differential and ephemeris estimation," *Journal of Guidance, Control, and Dynamics*, vol. 41, no. 1, pp. 268–275, 2017.

[6] D. Wang, H. He, and D. Liu, "Adaptive critic nonlinear robust control: A survey," *IEEE Transactions on Cybernetics*, vol. 47, no. 10, pp. 3429–3451, 2017.

[7] G. Wen, S. S. Ge, F. Tu, and Y. S. Choo, "Artificial potential-based adaptive H_∞ synchronized tracking control for accommodation vessel," *IEEE Transactions on Industrial Electronics*, vol. 64, no. 7, pp. 5640–5647, 2017.

[8] S.-L. Dai, S. He, H. Lin, and C. Wang, "Platoon formation control with prescribed performance guarantees for usvs," *IEEE Transactions on Industrial Electronics*, vol. 65, no. 5, pp. 4237–4246, 2017.

[9] Y. Song and X. Yuan, "Low-cost adaptive fault-tolerant approach for semiactive suspension control of high-speed trains," *IEEE Transactions on Industrial Electronics*, vol. 63, no. 11, pp. 7084–7093, 2016.

[10] D. Liu, Y. Xu, Q. Wei, and X. Liu, "Residential energy scheduling for variable weather solar energy based on adaptive dynamic programming," *IEEE/CAA Journal of Automatica Sinica*, vol. 5, no. 1, pp. 36–46, 2018.

[11] C. Yang, C. Zeng, P. Liang, Z. Li, R. Li, and C.-Y. Su, "Interface design of a physical human-robot interaction system for human impedance adaptive skill transfer," *IEEE Transactions on Automation Science & Engineering*, vol. 15, no. 1, pp. 329–340, 2018.

[12] Z. Gao, Q. Shi, T. Fukuda, C. Li, and Q. Huang, "An overview of biomimetic robots with animal behaviors," *Neurocomputing*, vol. 332, pp. 339–350, 2019.

[13] M. D. Zivanovic and M. Vukobratovic, *Multi-Arm Cooperating Robots: Dynamics and Control*. Dordrecht, Netherlands: Kluwer, Springer, 2006.

[14] J.-H. Jean and L.-C. Fu, "An adaptive control scheme for coordinated multimanipulator systems," *IEEE Transactions on Robotics & Automation*, vol. 9, no. 2, pp. 226–231, 1993.

[15] Z. Li, B. Huang, Z. Ye, M. Deng, and C. Yang, "Physical human–robot interaction of a robotic exoskeleton by admittance control," *IEEE Transactions on Industrial Electronics*, vol. 65, no. 12, pp. 9614–9624, 2018.

[16] W.-H. Zhu and J. De Schutter, "Control of two industrial manipulators rigidly holding an egg," *IEEE Control Systems*, vol. 19, no. 2, pp. 24–30, 1999.

[17] J. Luh and Y. Zheng, "Constrained relations between two coordinated industrial robots for motion control," *International Journal of Robotics Research*, vol. 6, no. 3, pp. 60–70, 1987.

[18] F. Caccavale, P. Chiacchio, A. Marino, and L. Villani, "Six-dof impedance control of dual-arm cooperative manipulators," *IEEE/ASME Transactions on Mechatronics*, vol. 13, no. 5, pp. 576–586, 2008.

[19] R. Bonitz and T. C. Hsia, "Internal force-based impedance control for cooperating manipulators," *IEEE Transactions on Robotics & Automation*, vol. 12, no. 1, pp. 78–89, 1996.

[20] C.-C. Hua and Y.-F. Chang, "Decentralized adaptive neural network control for mechanical systems with dead-zone input," *Nonlinear Dynamics*, vol. 76, no. 3, pp. 1845–1855, 2014.

[21] X. Chen, Y. Feng, and C.-Y. Su, "Adaptive control for continuous-time systems with actuator and sensor hysteresis," *Automatica*, vol. 64, pp. 196–207, 2016.

[22] H. Chen, L. Chen, Q. Zhang, and F. Tong, "Visual servoing of dynamic wheeled mobile robots with anti-interference finite-time controllers," *Assembly Automation*, vol. 38, no. 5, pp. 558–567, 2018.

[23] H. Wang, C. Wang, W. Chen, X. Liang, and Y. Liu, "Three-dimensional dynamics for cable-driven soft manipulator," *IEEE/ASME Transactions on Mechatronics*, vol. 22, no. 1, pp. 18–28, 2017.

[24] H. Wang, R. Zhang, W. Chen, X. Liang, and R. Pfeifer, "Shape detection algorithm for soft manipulator based on fiber bragg gratings," *IEEE/ASME Transactions on Mechatronics*, vol. 21, no. 6, pp. 2977–2982, 2016.

[25] Q. Shi, C. Li, K. Li, Q. Huang, H. Ishii, A. Takanishi, and T. Fukuda, "A modified robotic rat to study rat-like pitch and yaw movements," *IEEE/ASME Transactions on Mechatronics*, vol. 23, no. 5, pp. 2448–2458, 2018.

[26] C. Hua, G. Liu, L. Li, and X. Guan, "Adaptive fuzzy prescribed performance control for nonlinear switched time-delay systems with unmodeled dynamics," *IEEE Transactions on Fuzzy Systems*, vol. 26, no. 4, pp. 1934–1945, 2018.

[27] Q. C. Nguyen, M. Piao, and K.-S. Hong, "Multivariable adaptive control of the rewinding process of a roll-to-roll system governed by hyperbolic partial differential equations," *International Journal of Control, Automation and Systems*, vol. 16, no. 5, pp. 2177–2186, 2018.

[28] B. Gao and W. Han, "Neural network model reference decoupling control for single leg joint of hydraulic quadruped robot," *Assembly Automation*, vol. 38, no. 4, pp. 465–475, 2018.

[29] C. Hua, Y. Li, and X. Guan, "Finite/fixed-time stabilization for nonlinear interconnected systems with dead-zone input," *IEEE Transactions on Automatic Control*, vol. 62, no. 5, pp. 2554–2560, 2017.

[30] W. He, W. Ge, Y. Li, Y.-J. Liu, C. Yang, and C. Sun, "Model identification and control design for a humanoid robot," *IEEE Transactions on Systems, Man, and Cybernetics: Systems*, vol. 47, no. 1, pp. 45–57, 2017.

[31] X. Chen, C.-Y. Su, Z. Li, and F. Yang, "Design of implementable adaptive control for micro/nano positioning system driven by piezoelectric actuator," *IEEE Transactions on Industrial Electronics*, vol. 63, no. 10, pp. 6471–6481, 2016.

[32] W. He, Z. Li, and C. P. Chen, "A survey of human-centered intelligent robots: issues and challenges," *IEEE/CAA Journal of Automatica Sinica*, vol. 4, no. 4, pp. 602–609, 2017.

[33] D. Wang, H. He, and D. Liu, "Improving the critic learning for event-based nonlinear h_∞ control design," *IEEE Transactions on Cybernetics*, vol. 47, no. 10, pp. 3417–3428, 2017.

[34] G. Wen, S. S. Ge, and F. Tu, "Optimized backstepping for tracking control of strict-feedback systems," *IEEE Transactions on Neural Networks & Learning Systems*, vol. 29, no. 8, pp. 3850–3862, 2018.

[35] T. Meng and W. He, "Iterative learning control of a robotic arm experiment platform with input constraint," *IEEE Transactions on Industrial Electronics*, vol. 65, no. 1, pp. 664–672, 2017.

[36] S. S. Ge, T. H. Lee, and C. J. Harris, *Adaptive neural network control of robotic manipulators*, vol. 19. World Scientific, 1998.

[37] Y.-J. Liu, J. Li, S. Tong, and C. P. Chen, "Neural network control-based adaptive learning design for nonlinear systems with full-state constraints," *IEEE Transactions on Neural Networks & Learning Systems*, vol. 27, no. 7, pp. 1562–1571, 2016.

[38] G. Wen, C. P. Chen, Y.-J. Liu, and Z. Liu, "Neural network-based adaptive leader-following consensus control for a class of nonlinear multiagent state-delay systems," *IEEE Transactions on Cybernetics*, vol. 47, no. 8, pp. 2151–2160, 2017.

[39] C. Sun, W. He, W. Ge, and C. Chang, "Adaptive neural network control of biped robots," *IEEE Transactions on Systems, Man, and Cybernetics: Systems*, vol. 47, no. 2, pp. 315–326, 2017.

[40] C. Yang, X. Wang, L. Cheng, and H. Ma, "Neural-learning-based telerobot control with guaranteed performance," *IEEE Transactions on Cybernetics*, vol. 47, no. 10, pp. 3148–3159, 2017.

[41] S. Zhang, Y. Dong, Y. Ouyang, Z. Yin, and K. Peng, "Adaptive neural control for robotic manipulators with output constraints and uncertainties," *IEEE Transactions on Neural Networks & Learning Systems*, no. 99, pp. 1–11, 2018.

[42] P. Huang, D. Wang, Z. Meng, F. Zhang, and Z. Liu, "Impact dynamic modeling and adaptive target capturing control for tethered space robots with uncertainties," *IEEE/ASME Transactions on Mechatronics*, vol. 21, no. 5, pp. 2260–2271, 2016.

[43] M. Bianchini, P. Frasconi, and M. Gori, "Learning without local minima in radial basis function networks," *IEEE Transactions on Neural Networks & Learning Systems*, vol. 6, no. 3, pp. 749–756, 1995.

[44] Y. Li, S. Tong, and T. Li, "Hybrid fuzzy adaptive output feedback control design for uncertain mimo nonlinear systems with time-varying delays and input saturation," *IEEE Transactions on Fuzzy Systems*, vol. 24, no. 4, pp. 841–853, 2016.

[45] B. M. Chen, T. H. Lee, K. Peng, and V. Venkataramanan, "Composite nonlinear feedback control for linear systems with input saturation: Theory and an application," *IEEE Transactions on Automatic Control*, vol. 48, no. 3, pp. 427–439, 2003.

[46] Y. Li, S. Tong, and T. Li, "Composite adaptive fuzzy output feedback control design for uncertain nonlinear strict-feedback systems with input saturation," *IEEE Transactions on Cybernetics*, vol. 45, no. 10, pp. 2299–2308, 2015.

[47] W. Sun, Z. Zhao, and H. Gao, "Saturated adaptive robust control for active suspension systems," *IEEE Transactions on Industrial Electronics*, vol. 60, no. 9, pp. 3889–3896, 2013.

[48] C. Wen, J. Zhou, Z. Liu, and H. Su, "Robust adaptive control of uncertain nonlinear systems in the presence of input saturation and external disturbance," *IEEE Transactions on Automatic Control*, vol. 56, no. 7, pp. 1672–1678, 2011.

[49] Q. Zhou, L. Wang, C. Wu, H. Li, and H. Du, "Adaptive fuzzy control for nonstrict-feedback systems with input saturation and output constraint.," *IEEE Transactions on Systems, Man, and Cybernetics: Systems*, vol. 47, no. 1, pp. 1–12, 2017.

[50] H. Li, L. Wang, H. Du, and A. Boulkroune, "Adaptive fuzzy backstepping tracking control for strict-feedback systems with input delay," *IEEE Transactions on Fuzzy Systems*, vol. 25, no. 3, pp. 642–652, 2017.

[51] R. Cui, L. Chen, C. Yang, and M. Chen, "Extended state observer-based integral sliding mode control for an underwater robot with unknown disturbances and uncertain nonlinearities," *IEEE Transactions on Industrial Electronics*, vol. PP, no. 99, pp. 1–1, 2017.

[52] B. Xu and F. Sun, "Composite intelligent learning control of strict-feedback systems with disturbance," *IEEE Transactions on Cybernetics*, vol. 48, no. 2, pp. 730–741, 2018.

[53] W. He, X. He, and C. Sun, "Vibration control of an industrial moving strip in the presence of input deadzone," *IEEE Transactions on Industrial Electronics*, vol. 64, no. 6, pp. 4680–4689, 2017.

[54] Z. Zhang and S. Xu, "Observer design for uncertain nonlinear systems with unmodeled dynamics," *Automatica*, vol. 51, pp. 80–84, 2015.

[55] W. He, S. S. Ge, and D. Huang, "Modeling and vibration control for a nonlinear moving string with output constraint," *IEEE/ASME Transactions on Mechatronics*, vol. 20, no. 4, pp. 1886–1897, 2015.

[56] B. Xu, D. Wang, Y. Zhang, and Z. Shi, "Dob based neural control of flexible hypersonic flight vehicle considering wind effects," *IEEE Transactions on Industrial Electronics*, vol. 64, no. 11, pp. 8676–8685, 2017.

[57] H. Li, Y. Gao, P. Shi, and H.-K. Lam, "Observer-based fault detection for nonlinear systems with sensor fault and limited communication capacity," *IEEE Transactions on Automatic Control*, vol. 61, no. 9, pp. 2745–2751, 2016.

[58] Z. Li, C.-Y. Su, L. Wang, Z. Chen, and T. Chai, "Nonlinear disturbance observer-based control design for a robotic exoskeleton incorporating fuzzy approximation," *IEEE Transactions on Industrial Electronics*, vol. 62, no. 9, pp. 5763–5775, 2015.

[59] Z. Li, Y. Kang, Z. Xiao, and W. Song, "Human–robot coordination control of robotic exoskeletons by skill transfers," *IEEE Transactions on Industrial Electronics*, vol. 64, no. 6, pp. 5171–5181, 2017.

[60] M. Chen and S. S. Ge, "Direct adaptive neural control for a class of uncertain nonaffine nonlinear systems based on disturbance observer," *IEEE Transactions on Cybernetics*, vol. 43, no. 4, pp. 1213–1225, 2013.

[61] L. Guo and W.-H. Chen, "Disturbance attenuation and rejection for systems with nonlinearity via dobc approach," *International Journal of Robust and Nonlinear Control: IFAC-Affiliated Journal*, vol. 15, no. 3, pp. 109–125, 2005.

[62] W.-H. Chen, D. J. Ballance, P. J. Gawthrop, and J. O'Reilly, "A nonlinear disturbance observer for robotic manipulators," *IEEE Transactions on Industrial Electronics*, vol. 47, no. 4, pp. 932–938, 2000.

[63] G. Feng, "Stability analysis of discrete-time fuzzy dynamic systems based on piecewise lyapunov functions," *IEEE Transactions on Fuzzy Systems*, vol. 12, no. 1, pp. 22–28, 2004.

[64] P. Liu, Z. Zeng, and J. Wang, "Multiple mittag–leffler stability of fractional-order recurrent neural networks," *IEEE Transactions on Systems, Man, and Cybernetics: Systems*, vol. 47, no. 8, pp. 2279–2288, 2017.

[65] A. Wu and Z. Zeng, "Global mittag–leffler stabilization of fractional-order memristive neural networks," *IEEE transactions on neural networks and learning systems*, vol. 28, no. 1, pp. 206–217, 2015.

[66] E. Kim and D. Kim, "Stability analysis and synthesis for an affine fuzzy system via lmi and ilmi: Discrete case," *IEEE Transactions on Systems, Man, and Cybernetics, Part B (Cybernetics)*, vol. 31, no. 1, pp. 132–140, 2001.

[67] S. Hayati, "Hybrid position/force control of multi-arm cooperating robots," in *Robotics and Automation. Proceedings. 1986 IEEE International Conference on*, vol. 3, pp. 82–89, IEEE, 1986.

[68] W. He, S. S. Ge, Y. Li, E. Chew, and Y. S. Ng, "Neural network control of a rehabilitation robot by state and output feedback," *Journal of Intelligent & Robotic Systems*, vol. 80, no. 1, pp. 15–31, 2015.

[69] W. Gueaieb, F. Karray, and S. Al-Sharhan, "A robust adaptive fuzzy position/force control scheme for cooperative manipulators," *IEEE Transactions on Control Systems Technology*, vol. 11, no. 4, pp. 516–528, 2003.

[70] C. Yang, Y. Jiang, Z. Li, W. He, and C.-Y. Su, "Neural control of bimanual robots with guaranteed global stability and motion precision," *IEEE Transactions on Industrial Informatics*, vol. 13, no. 3, pp. 1162–1171, 2017.

[71] S. S. Ge and C. J. Harris, *Adaptive Neural Network Control of Robotic Manipulators*. World Scientific Publishing Co., Inc., 1998.

[72] S. S. Ge, C. C. Hang, T. H. Lee, and T. Zhang, *Stable Adaptive Neural Network Control*. Boston, MA, USA: Kluwer, 2001.

[73] V. Santibañez, K. Camarillo, J. Moreno-Valenzuela, and R. Campa, "A practical pid regulator with bounded torques for robot manipulators," *International Journal of Control, Automation & Systems*, vol. 8, no. 3, pp. 544–555, 2010.

[74] K. J. Åström and T. Hägglund, *PID controllers: theory, design, and tuning*, vol. 2. Instrument society of America Research Triangle Park, NC, 1995.

[75] S. Seshagiri and H. K. Khalil, "Output feedback control of nonlinear systems using rbf neural networks," *IEEE Transactions on Neural Networks & Learning Systems*, vol. 11, no. 1, pp. 69–79, 2000.

[76] V. Chandwani, V. Agrawal, and R. Nagar, "Modeling slump of ready mix concrete using genetic algorithms assisted training of artificial neural networks," *Expert Systems with Applications*, vol. 42, no. 2, pp. 885–893, 2015.

[77] L. Cheng, W. Liu, Z.-G. Hou, J. Yu, and M. Tan, "Neural-network-based nonlinear model predictive control for piezoelectric actuators," *IEEE Transactions on Industrial Electronics*, vol. 62, no. 12, pp. 7717–7727, 2015.

Wei He (S'09–M'12–SM'16) received the B.Eng. degree in automation and the M.Eng. degree in control science and engineering from the College of Automation Science and Engineering, South China University of Technology, Guangzhou, China, in 2006 and 2008, respectively, and the Ph.D. degree in control science and engineering from the Department of Electrical and Computer Engineering, National University of Singapore, Singapore, in 2011.

He is currently a Full Professor with the School of Automation and Electrical Engineering, University of Science and Technology Beijing, Beijing, China. He has coauthored 2 books published in Springer and published over 100 international journal and conference papers. His current research interests include robotics, distributed parameter systems, and intelligent control systems.

Dr. He was a recipient of the Newton Advanced Fellowship from the Royal Society, U.K., in 2017 and the IEEE SMC Society Andrew P. Sage Best Transactions Paper Award in 2017. He is serving the Chair of IEEE SMC Society Beijing Capital Region Chapter. He is serving as an Associate Editor for the IEEE TRANSACTIONS ON NEURAL NETWORKS AND LEARNING SYSTEMS, IEEE TRANSACTIONS ON CONTROL SYSTEMS TECHNOLOGY, IEEE TRANSACTIONS ON SYSTEMS, MAN, AND CYBERNETICS: SYSTEMS, IEEE/CAA JOURNAL OF AUTOMATICA SINICA, and Neurocomputing, and an Editor of the Journal of Intelligent and Robotic Systems.

Yongkun Sun received the B.E. degree in automation from the School of Automation and Electrical Engineering, University of Science and Technology Beijing, Beijing, China, in 2017 and now he is working toward the M.E. degree at University of Science and Technology Beijing. His research interests include intelligent control, neural networks, and robotics.

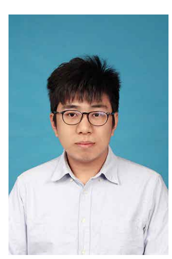

Zichen Yan (S'16) received the B.E. and M.E. degrees from the School of Automation and Electrical Engineering, University of Science and Technology Beijing, Beijing, China, in 2015 and 2018, respectively, where he is currently pursuing the Ph.D. degree.

His current research interests include intelligent control, neural networks, and robotics.

Chenguang Yang (M'10–SM'16) received the B.Eng. degree in measurement and control from Northwestern Polytechnical University, Xi'an, China, in 2005, and the Ph.D. degree in control engineering from the National University of Singapore, Singapore, in 2010.

He is a Professor of Robotics with the University of the West of England, Bristol, U.K. He was a Post-Doctoral Fellow with Imperial College London, London, U.K., from 2009 to 2010. His current research interests include human–robot interaction and intelligent system design.

Dr. Yang was a recipient of the Marie Curie International Incoming Fellowship Award, the EPSRC Innovation Fellowship, and the Best Paper Award of the IEEE TRANSACTIONS ON ROBOTICS as well as over ten conference best paper awards.

Zhijun Li (M'07–SM'09) received the Ph.D. degree in mechatronics, Shanghai Jiao Tong University, Shanghai, China, in 2002.

From 2003 to 2005, he was a Post-Doctoral Fellow with the Department of Mechanical Engineering and Intelligent Systems, University of Electro-Communications, Tokyo, Japan. From 2005 to 2006, he was a Research Fellow with the Department of Electrical and Computer Engineering, National University of Singapore, Singapore, and Nanyang Technological University, Singapore. Since 2012, he has been a Professor with the College of Automation Science and Engineering, South China University of Technology, Guangzhou, China. Since 2017, he has been a Professor with the Department of Automation, University of Science and Technology, Hefei, China. His current research interests include wearable robotics, tele-operation systems, nonlinear control, and neural network optimization.

Dr. Li has been the Co-Chair of IEEE SMC Technical Committee on Bio-Mechatronics and Bio-Robotics Systems, and IEEE-RAS Technical Committee on Neuro-Robotics Systems in 2016. He is serving as an Editor-at-Large of Journal of Intelligent & Robotic Systems and an Associate Editor of several IEEE TRANSACTIONS.

Okyay Kaynak (SM'90–F'03) received the B.Sc. degree with first class honors and Ph.D. degrees in electronic and electrical engineering from the University of Birmingham, UK, in 1969 and 1972 respectively. From 1972 to 1979, he held various positions within the industry. In 1979, he joined the Department of Electrical and Electronics Engineering, Bogazici University, Istanbul, Turkey, where he is currently a Professor Emeritus, holding the UNESCO Chair on Mechatronics. He is also a 1000 People Plan Professor at University of Science & Technology Beijing, China. He has hold long-term (near to or more than a year) Visiting Professor/Scholar positions at various institutions in Japan, Germany, U.S., Singapore and China. His current research interests are in the fields of intelligent control and mechatronics. He has authored three books, edited five and authored or co-authored more than 400 papers that have appeared in various journals and conference proceedings.

Dr. Kaynak has served as the Editor in Chief of IEEE Trans. on Industrial Informatics and IEEE/ASME Trans. on Mechatronics as well as Co- Editor in Chief of IEEE Trans. on Industrial Electronics. Additionally, he is on the Editorial or Advisory Boards of a number of scholarly journals. He recently received the Chinese Government's Friendship Award and Humboldt Research Prize (both in 2016).

Dr. Kaynak is active in international organizations, has served on many committees of IEEE and was the president of IEEE Industrial Electronics Society during 2002-2003. He was elevated to IEEE fellow status in 2003.